Current Biology, Vol. 12, 454–466, March 19, 2002, ©2002 Elsevier Science Ltd. All rights reserved. PII S0960-9822(02)00723-6

An Evolutionary Conserved Region in the *vasa* 3′UTR Targets RNA Translation to the Germ Cells in the Zebrafish

Holger Knaut,[1,4] Herbert Steinbeisser,[2] Heinz Schwarz,[3] and Christiane Nüsslein-Volhard[1]
[1]Abteilung III/Genetik
[2]Abteilung V/Zellbiologie und
[3]Elektronenmikroskopie Labor
Max Planck Institut für Entwicklungsbiologie
Spemannstrasse 35
72076 Tübingen
Germany

Summary

Background: In many animals, germ cells are set aside from somatic cells early during development to give rise to sperm in males and eggs in females. One strategy to achieve this separation is to localize special cytoplasmic granules to the precursors of the germline. In *Drosophila*, the *vasa* gene has been shown to encode an essential component of these granules. While Vasa protein is directly targeted to the forming germ cells of *Drosophila*, Vasa protein expression in the germline of *Xenopus* and zebrafish is thought to be achieved by RNA localization.

Results: To analyze whether the machinery responsible for RNA localization is conserved among lower vertebrates, we tested different *vasa* homologs for their ability to localize in *Xenopus* oocytes. Reporter transcripts fused to the *vasa* 3′UTR of zebrafish are recruited to the germ plasm of injected *Xenopus* oocytes, although the 3′UTR shows no clear sequence similarity to the *Xenopus vasa*-like DEADsouth 3′UTR. However, isolation, expression pattern analysis, and sequence inspection of *vasa* genes from different teleosts indicate that RNA localization correlates with the presence of several conserved regions in the 3′UTR. Introduction of reporter transcripts fused to different *vasa* 3′UTR deletions into *Xenopus* and zebrafish demonstrates that one of these conserved regions is sufficient for RNA localization in either species. Moreover, these regions target GFP translation to the germline of transgenic fish.

Conclusions: Our results suggest the existence of a common RNA localization machinery in lower vertebrates that uses a functionally conserved localization signal to target gene expression to the germline.

Introduction

Primordial germ cells (PGCs) are cells that will differentiate into gametes, forming the sperm in males and the eggs in females. They are responsible for transmitting genetic information between generations. Early in development, they segregate from the somatic cells following a distinct cell division pattern and migrate through the embryo to the future site of the gonads. The factors that distinguish PGCs from somatic cells are not known completely, nor do we fully understand the process of PGC migration to and coalescence with the gonadal tissue. In many animals, the PGCs inherit a special cytoplasm, the germ plasm, that distinguishes these cells from somatic cells. This germ plasm consists of granules associated with fibrils and mitochondria. One component that has been identified in the germ cells of all animal species analyzed to date is the product of the *vasa* gene. *vasa* was initially identified by genetic screens in *Drosophila* as a maternal-effect gene required for germ cell formation [1] and has since been shown to encode an RNA helicase of the DEAD box family [2, 3]. In *Drosophila* and *Caenorhabditis*, *vasa* loss of function leads to defective oogenesis, and, in mouse, targeted deletion of the *vasa* gene results in defective spermatogenesis (reviewed in [4, 5]).

In *Drosophila*, the Vasa protein is segregated to the posterior pole of the oocyte as a component of the germ plasm. After egg deposition, Vasa protein and germ plasm are directly incorporated into the pole cells, the PGCs of *Drosophila* [2, 3, 6]. Similar to *Drosophila*, the four Vasa-like proteins of *Caenorhabditis* (glh-1 to -4) are also components of the germ plasm and are required for germline development [7, 8]. During the first four cell divisions, these Vasa-like proteins and the germ plasm asymmetrically segregate to the founder cell of the *Caenorhabditis* germline [7–10].

In contrast to *Drosophila* and *Caenorhabditis*, in *Xenopus* and zebrafish it is the *vasa* RNA and not the Vasa protein that is a component of the germ plasm [11–14]. In *Xenopus*, the RNA of the *vasa*-like gene *DEADsouth* is localized to the granules of the germ plasm at the vegetal pole of oocytes and is segregated to the four vegetal cells during the initial cell divisions [14]. Zebrafish *vasa* RNA is also localized to germ plasm granules, but these granules are associated with the cortex of the animal pole of late-stage oocytes [13]. Strikingly, during the first two cleavage divisions in zebrafish embryos, *vasa* RNA granules are concentrated to the distal parts of the cleavage furrows, resulting in four *vasa* RNA containing aggregates [11–13]. These aggregates are asymmetrically segregated during every cell division such that only four PGCs are present in the late zebrafish blastula. Shortly before gastrulation, these four cells begin to divide symmetrically and start to migrate to the future site of the gonads [11, 13, 15–17, 25].

In order to investigate the *cis*-acting factors required for RNA localization, we have isolated the *vasa* genes from several fish species and analyzed their RNA expression patterns. We find that species belonging to the ostariophysan clade (which includes zebrafish) localize *vasa* RNA to the germ plasm, and those of the euteleost clade (which include medaka) do not. By comparing the sequences of the 3′UTRs from each species, we were able to identify several conserved elements which are present only in those species which localize *vasa* RNA. Using GFP as a reporter, we dissected the zebrafish *vasa* 3′UTR and show that one of the conserved elements

[4]Correspondence: holger.knaut@tuebingen.mpg.de

confers germ plasm localization in both zebrafish and *Xenopus*. In agreement, we find that the ostariophysan *vasa* 3′UTRs which contain this element are sufficient for RNA localization, while the euteleost *vasa* 3′UTRs which lack this element are not. Furthermore, we find that *vasa* RNA also localizes to the germ plasm in butterfly fish, a basal teleost species, and that its 3′UTR also is sufficient for this localization in injected *Xenopus* oocytes. Based on these observations, we draw three conclusions. First, *vasa* RNA localization to the germ plasm appears to be an ancesteral feature in fish and frog that depends on a functional localization element in the 3′UTR. Second, loss of this localization element during euteleost evolution is a likely explanation for the lack of localized *vasa* RNA. Third, the machinery responsible for this RNA localization is conserved between fish and frog. Moreover, we use the germ plasm localization signal within the *vasa* 3′UTR to localize and translate GFP RNA in the germline of transgenic zebrafish, allowing us to study PGCs in live zebrafish.

Results

vasa RNA Localization in Teleosts Correlates with Conserved Elements in Its 3′UTR

To address the question how *vasa* RNA is selectively recognized in the oocyte and assembled into the germ plasm, we searched for the region within the *vasa* RNA that is responsible for germ plasm localization. As a first step toward this end, we used in situ hybridization to test whether localization of *vasa* RNA in medaka (*Oryzias latipes*) resembles that of zebrafish. To our surprise, medaka *vasa* RNA is not localized during oogenesis or early embryogenesis, although it is later specifically expressed in the PGCs of 7 somite stage embryos (Figures 1Ak and 1Al and [26]). To understand the difference in *vasa* RNA localization between zebrafish and medaka, we isolated and compared *vasa* transcripts of six additional teleost species. The species analyzed were chosen such that the main clades of the phylogenetic tree of the teleosts are covered. Of these six species the freshwater butterfly fish (*Pantodon buchholzi*) represents the most basal species. Tetra (*Hyphessobryon ecuadoriensis*), carp (*Cyprinus carpio*) and Fegrade's danio (*Danio feegradei*) are representatives of the ostariophysan clade, and trout (*Oncorhynchus mykiss*) and rainbow fish (*Melanotaenia fluviatilis*) together with medaka belong to the euteleost clade. The above described phylogenetic relationship is based on morphological studies [27] and is supported by the evolutionary distances calculated for the *vasa* coding sequences from the analyzed fish species (Figure 1Am).

To test if *vasa* RNA is distributed in a localized pattern in these additional six species, ovaries and embryos were stained for *vasa* RNA. In ostariophysans (Fegrade's danio, carp, and tetra), *vasa* RNA is localized in blastula stage embryos to four subcellular clusters that are later found specifically in presumptive PGCs (Figures 1Aa–1Ad, 1Ag, and 1Ah). The localization pattern is identical to the *vasa* RNA distribution during zebrafish embryogenesis [11, 12]. Similar to medaka, the other two euteleosts (trout and rainbow fish) do not localize *vasa* RNA in blastula stage embryos (Figures 1Ai and 1Aj). The localization pattern of *vasa* transcripts in post blastula stage rainbow fish and trout could not be analyzed due to the lack of embryos. However, a recent study showed that *vasa* transcripts are specifically present in presumptive PGCs in 80 somite stage trout embryos [28]. Importantly, in freshwater butterfly fish, the most basal teleost species analyzed, *vasa* transcripts are localized during oogenesis similar to the pattern seen in ostariophysan oocytes (Figure 1Bd, compare to zebrafish oocyte in Figure 1Ba and to medaka oocyte in Figure 1Bg).

Since *vasa* RNA is recruited to the zebrafish germ plasm and the germ plasm is localized subcellularly during oogenesis [13], localization of *vasa* RNA in butterfly fish oocytes suggests that butterfly fish *vasa* RNA is also recruited to the germ plasm and presumably localized during embryonic cleavage stages. In support of this suggestion, we find *vasa* RNA during butterfly fish oogenesis in electron-dense structures that may represent the precursors of the forming germ plasm. In contrast, we failed to detect subcellular *vasa* RNA localization in medaka oocytes, although germ plasm is present [40] (Figure 1Bh, compare to butterfly fish oocyte in Figure 1Be and to zebrafish oocyte in Figure 1Bb). Moreover, we find *vasa* RNA expression restricted to a subset of cells in pregastrulation embryos of both ostariophysans and butterfly fish but not medaka (Figures 1Bc, 1Bc′, 1Bf, and 1Bf′, compare to medaka embryo in Figures 1Bi and 1Bi′). From these observations, we conclude that *vasa* RNA localization is a basal feature in teleosts and that euteleosts have lost the ability to localize *vasa* RNA.

To investigate if the ability to localize *vasa* transcripts correlates with conserved sequence elements, we compared the sequences of (localized) ostariophyan *vasa* RNAs with those of (nonlocalized) euteleost *vasa* RNAs. The most striking differences reside within the 3′UTRs of the two sets of transcripts analyzed. While the *vasa* coding sequences are highly conserved, the *vasa* 3′UTRs from medaka, rainbow fish, and freshwater butterfly fish are half the length of the 3′UTRs from trout and the ostariophysans. Accordingly, we find the degree of nucleotide identity between zebrafish and the ostariophysan *vasa* 3′UTR higher than between zebrafish and the euteleost *vasa* 3′UTR (Table 1 and Figure 2). In accordance with that observation, the sequence alignment of *vasa* 3′UTRs from the ostariophysan species (tetra, carp, and Fegrade's danio) to the *vasa* 3′UTR of zebrafish shows stretches of moderate to high sequence conservation which is not found in the *vasa* 3′UTRs of the euteleosts analyzed (Figure 2). To test whether this conservation in sequence also is reflected in conserved secondary structures, we used the Zuker RNA folding program MFOLD [19] to predict the secondary structure of all four ostariophysan *vasa* 3′UTRs. Based on these predictions, the analyzed 3′UTRs share four stretches of similar secondary structure (Figure 2), suggesting that they might be involved in *vasa* RNA localization.

Euteleost but Not Ostariophysan *vasa* RNAs Lack a Functional Germ Plasm Localization Element

In order to test if the ability to localize *vasa* transcripts depends on the 3′UTR, we used the *Xenopus* oocyte

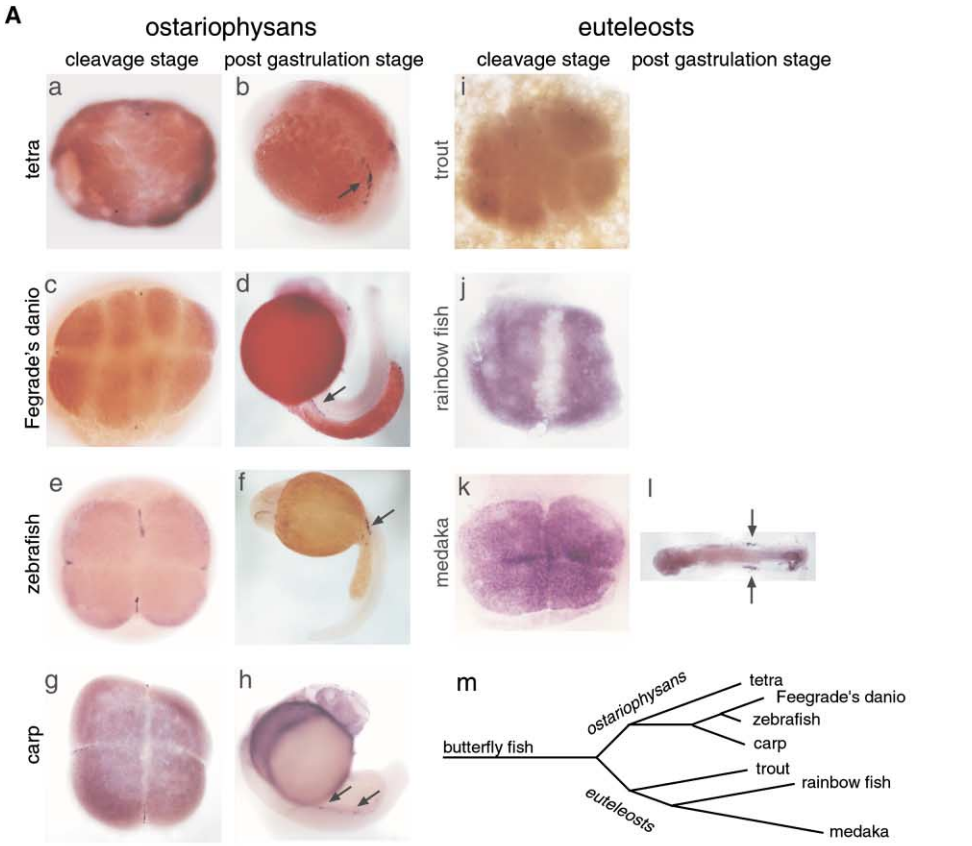

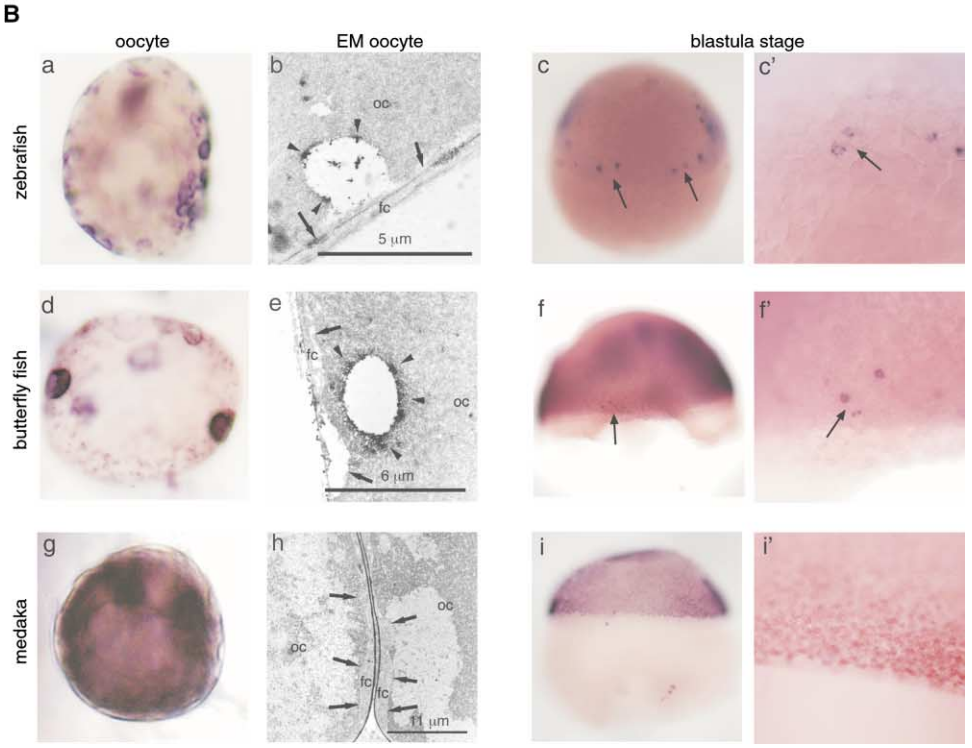

Figure 1. *vasa* RNA Localization in Teleosts Visualized by Whole-Mount In Situ Hybridization

(A) The phylogenetic relationship of the studied teleost species is shown in the lower part of the figure (Am). The phylogeny is based on the Vasa protein coding sequences, and distances between branch points and individual fish species are proportional to the calculated evolutionary distances. The teleosts fall into two main clades: the ostariophysans and the euteleosts. Ostariophysan fish localize *vasa* RNA subcellularly during blastula and early embryonic stages as seen for tetra ([Aa], 32 cell embryo, note that only two of the four *vasa* RNA aggregates are in

Table 1. Comparison of Teleost Vasa Proteins and *vasa* 3′UTRs

Species	Percent Identity to Zebrafish Vasa Protein (%)	Percent Identity to Zebrafish *vasa* 3′UTR (%)	Length of 3′UTR (bases)
zebrafish	100	100	645
Fegrade's danio	97	80	593
carp	95	60	634
tetra	87	48	621
trout	82	42	614
butterfly fish	83	38	327
rainbow fish	78	18	305
medaka	77	13	243

Note: Sequence comparison of *vasa* 3′UTR with unrelated 3′UTRs yields 18%–29% identity; purely stochastic alignments should yield 25% identity on average.

injection assay based on the assumption that the RNA localization machinery in zebrafish and *Xenopus* might be conserved. Indeed, we find that injection of reporter gene transcripts fused to zebrafish *vasa* 3′UTR localize to the vegetal pole of *Xenopus* oocytes, while control injections of reporter gene transcripts fused to the unrelated SV40 poly A signal do not localize (Figures 3A and 3G–3I). To demonstrate that reporter gene transcripts fused to *vasa* 3′UTR do not merely localize to the vegetal pole but also are incorporated into the *Xenopus* germ plasm, we sectioned injected ovaries stained for reporter transcripts using an electron-dense substrate. Inspection of ultrathin sections shows that injected reporter gene *vasa* 3′UTR fusion transcripts are associated with the mitochondrial cloud of the *Xenopus* germ plasm, while injection of GFP transcripts fused to the SV40 poly A signal do not enrich in this structure (Figures 3J and 3O). These results demonstrate that the zebrafish *vasa* 3′UTR confers the ability to localize RNA to the germ plasm and that the RNA recruiting machinery is functionally conserved between *Xenopus* and zebrafish.

To test if the ability to localize *vasa* transcripts depends on the conserved sequence elements present in ostariophysan but not euteleost *vasa* 3′UTRs, we injected reporter transcripts fused to the different teleost *vasa* 3′UTRs into *Xenopus* oocytes and scored for their ability to localize reporter transcripts. Whereas reporter gene transcripts fused to *vasa* 3′UTRs from ostariophysans and the more basal butterfly fish localize to the vegetal pole (Figures 3A, 3H, 3I, 3M, 3N, 3R, and 3S and Table 2), *vasa* 3′UTRs from euteleosts do not localize the reporter (Figures 3A and 3U and Table 2). These observations demonstrate that euteleosts do not possess a functional localization element and suggest that the lack of *vasa* RNA localization in this clade is due to the loss of a localization element in the euteleost *vasa* 3′UTRs.

To investigate the functional significance of the conserved domains in ostariophysan *vasa* 3′UTRs, we tested systematic deletions of the zebrafish *vasa* 3′UTR for their ability to localize reporter transcripts in injected *Xenopus* oocytes. We find that reporter transcripts that are fused to the first 334 nucleotides (elements 1 and 2), to nucleotides 157 to 642 (elements 2 to 4), or nucleotides 157 to 334 (element 2) of zebrafish *vasa* 3′UTR localize to the vegetal pole of *Xenopus* oocytes (Figures 3A, 3L, and 3Q and data not shown). In contrast, GFP transcripts fused to the first 141 nucleotides (element 1) or nucleotides 362 to 642 (elements 3 and 4) of *vasa* 3′UTR do not localize (Figure 3A). These results show that a 180 nucleotide element which encompasses the second conserved region of the zebrafish *vasa* 3′UTR is sufficient for localization to the *Xenopus* germ plasm.

Since the *Xenopus* RNA recruiting machinery is capable of localizing this conserved 180 nucleotide element, we searched for regions of homologies to this 180 nucleotide element in the 3′UTR of *Xenopus vasa*-like gene *DEADsouth* [29]. We identified weak homologies to the zebrafish *vasa* RNA localization element clustered over a 450 nucleotide region in the 1500 nucleotide 3′UTR of *DEADsouth*. Although we do not detect significant similarities on the secondary structure level between the zebrafish 180 nucleotide element and the 450 nucleotides in the *Xenopus* DEADsouth RNA, injection of re-

the plane of focus, and [Ab], 20 hpf embryo), Fegrade's Danio ([Ac], 8 cell embryo and [Ad], 30 hpf embryo), zebrafish ([Ae], 4 cell embryo and [Af], 36 hpf embryo), and carp ([Ag], 4 cell embryo and [Ah], 24 hpf embryo). In contrast to ostariophysans, euteleost fish do not localize *vasa* RNA during blastula stages, although *vasa* RNA expression is restricted during later embryogenesis to presumptive PGCs. This is seen in trout ([Ai], 8 cell embryo), rainbow fish ([Aj], 2 cell embryo), and medaka ([Ak], 4 cell embryo and [Al], 7 somite embryo). Arrows indicate PGCs.

(B) In the freshwater butterfly fish, a basal teleost species, *vasa* RNA is localized in oocytes (Bd and Be) similar to zebrafish stage II oocytes (Ba and Bb) both in whole-mount in situ hybridization and on an ultrastructural level. This localization pattern is not detected in oocytes of the euteleost medaka ([Bg and Bh] [26], note oocyte in [Bg] is strongly stained to detect weak localized signals). In agreement, restriction of *vasa* RNA expression to a subset of cells in pregastrulation butterfly fish embryos ([Bf], dome to 30% epiboly embryo, magnification in [Bf′]) resembles the expression pattern in zebrafish embryos ([Bc], dome to 30% epiboly embryo, magnification [Bc′]) and contrasts the ubiquitous expression of *vasa* RNA in medaka ([Bi], dome to 30% epiboly embryo, magnification in [Bi′]). Arrowheads point to subcellular *vasa* RNA signals in [Bb], [Be], and [Bh]. Arrows indicate the follicle cell (fc)-oocyte (oc) border in [Bb], [Be], and [Bf] and PGCs in [Bc], [Bc′], [Bf], and [Bf′].

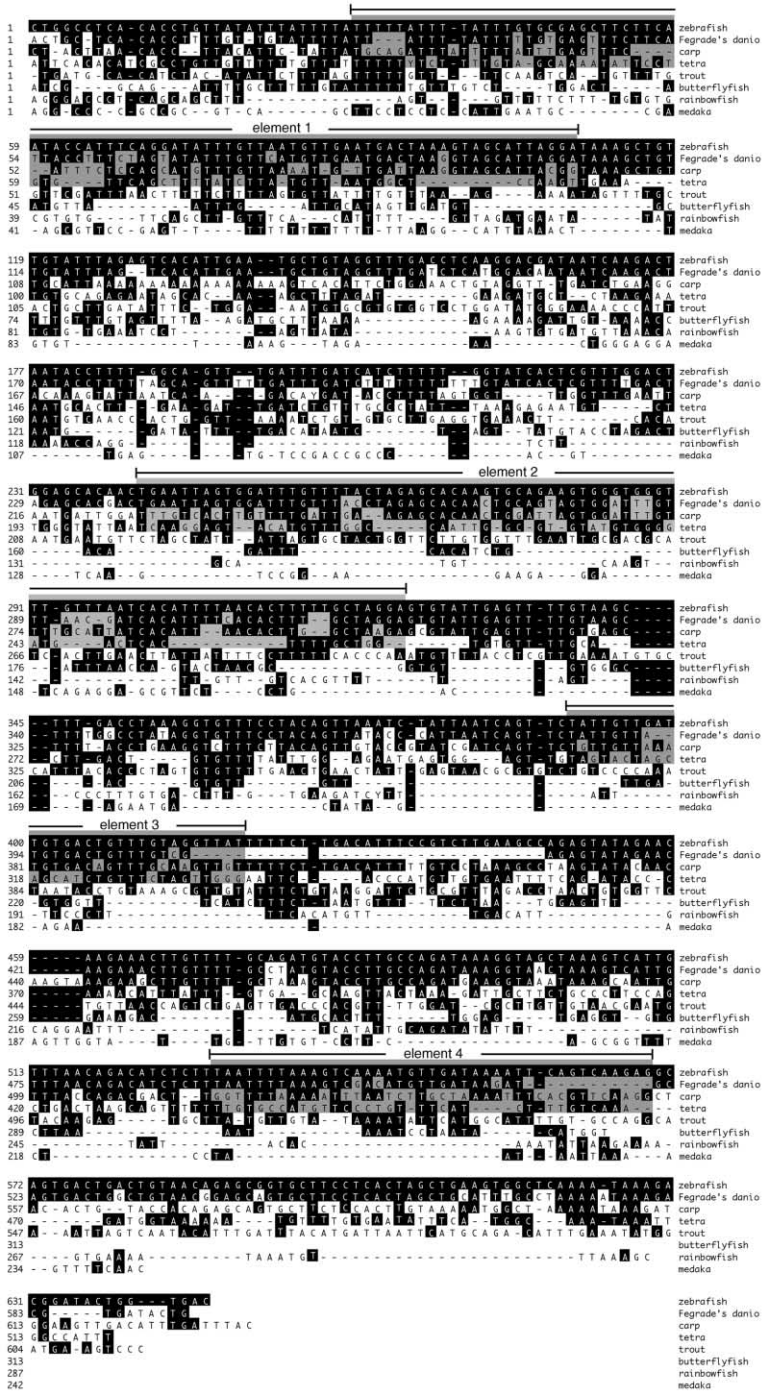

Figure 2. Teleost *vasa* 3′UTR Sequence Comparison

The zebrafish [11, 12], Fegrade's Danio [13], carp (this work), tetra (this work), trout (this work, [28]), butterfly fish (this work), rainbow fish (this work), and medaka (this work, [26]) *vasa* 3′UTRs sequences are aligned. Nucleotides that are identical to the zebrafish *vasa* 3′UTR are shaded in black. Sequence intervals that fold into similar secondary structures are shaded in gray and are named elements 1 through 4. The sequences are arranged according to their evolutionary distances to zebrafish.

porter transcripts fused to this 450 nucleotide region also leads to vegetal localization of reporter transcripts. This demonstrates that a functional localization element is present within these 450 nucleotides (Figure 3A).

To test if the *vasa* 3′UTR localization element is also recognized by localization machineries in invertebrates, we expressed the zebrafish *vasa* gene in *Drosophila* ovaries. While the zebrafish *vasa* RNA and protein are detectable in transgenic *Drosophila* ovaries, neither the transcript nor the protein is localized. This indicates that the germ plasm RNA localization machinery or at least some crucial elements in the machinery are not conserved in invertebrates (data not shown).

A 340 Nucleotide Element in the *vasa* 3′UTR Encompassing the 180 Nucleotide Localization Element Is Sufficient to Target GFP Expression to the Zebrafish Germline

To test if *vasa* 3′UTR is also required for localization and translation of *vasa* RNA in the zebrafish germline,

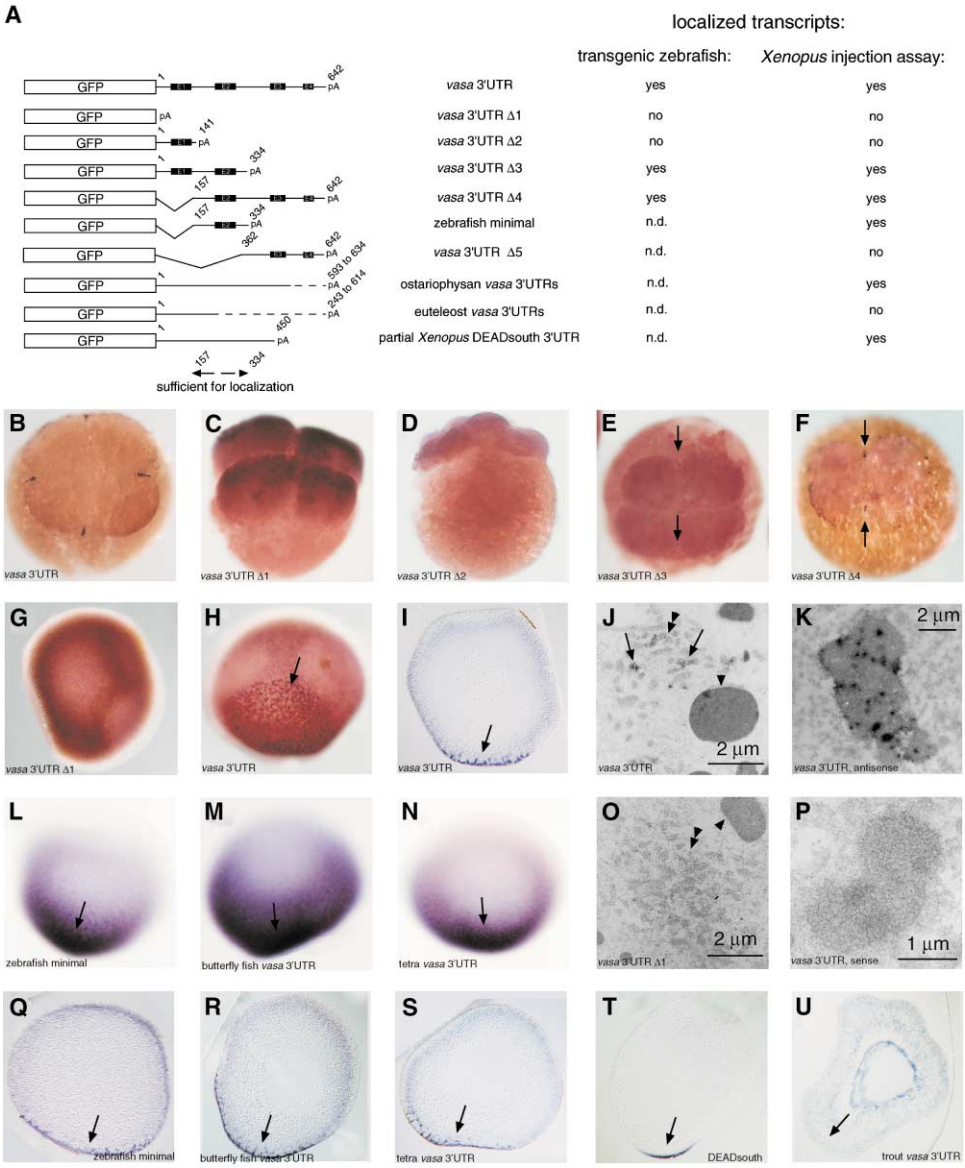

Figure 3. Constructs Used to Analyze the *vasa* 3′UTR of Teleosts and *Xenopus*

(A) GFP reporter gene constructs fused to zebrafish *vasa* 3′UTR deletion mutants and to *vasa* 3′UTRs from different teleost species and *Xenopus* are depicted. The ability of these 3′UTRs to localize the GFP reporter gene transcripts in transgenic zebrafish (first column) and in the *Xenopus* oocyte injection assay (second column) is shown. The ability to localize transcripts in transgenic zebrafish and in the *Xenopus* oocyte injection assay is denoted with "yes" or "no." A 180 nucleotide region sufficient for localization is indicated with an arrow underneath the different GFP reporter gene constructs and is refered to as the zebrafish *vasa* RNA localization element. Ostariophysan *vasa* 3′UTRs include Fegrade' danio and tetra, while euteleost *vasa* 3′UTRs include trout, rainbowfish, and medaka. Nucleotide numbers above the expressed transcripts are indicated, 1 being the first nucleotide after the stop codon. Conserved secondary structure elements in the zebrafish *vasa* 3′UTR are indicated as boxes E1 to 4. n.d., not done.

(B–F) Whole-mount in situ hybridization against GFP transcripts in early blastula stages from transgenic zebrafish. Zebrafish *vasa* 3′UTR constructs that contain nucleotides 157 to 334, the zebrafish *vasa* RNA localization element, localize to the germ plasm (B, E, F, and K), while constructs lacking that region show no localization (C and D).

(G–U) Whole-mount in situ hybridization against antisense GFP transcripts (but in [T], which is hybridized against antisense *Xenopus DEADsouth* RNA, and in [P], which is hybridized against sense GFP) in injected and cultured *Xenopus* oocytes, 10 μm sections of these oocytes (I and Q–U) and whole-mount in situ hybridization against GFP transcripts in 4 cell transgenic zebrafish embryos (K and P). Injection of GFP RNA fused to the SV40 poly A signal shows no vegetal localization (G), while injection of GFP RNA fused to zebrafish *vasa* 3′UTR shows localization at the vegetal cortex (H and I) similar to the cortical localization of the endogenous germ plasm component *DEADsouth* (T). Ultrathin sections through *Xenopus* oocytes injected with GFP RNA fused to *vasa* 3′UTR and stained with an electron-dense substrate show that these transcripts associate with the mitochondrial cloud (J). Similarly, maternally expressed GFP RNA-*vasa* 3′UTR fusion transcripts in transgenic zebrafish associate with the germ plasm (compare hybridization against antisense GFP in [K] with hybridization against sense GFP in [P]). Injection of GFP RNA-SV40 poly A signal fusion transcripts are not localized to the mitochondrial cloud (O). Injection of GFP RNA fused to the nucleotides 157 to 334 of the zebrafish *vasa* 3′UTR, to *vasa* 3′UTRs from butterfly fish or tetra show localization to the cortex at the vegetal pole ([L–N and Q–S], arrows indicate GFP RNA positive cortical granules), while GFP RNA fused to the *vasa* 3′UTR from trout shows no cortical localization (U). Arrows indicate germinal granules (J and O) or vegetal pole (I and Q–U), arrowheads point to yolk platelets, and double arrowheads indicate mitochondria.

Table 2. Comparison of the Ability of Teleost and *Xenopus vasa* 3′UTRs and Zebrafish *vasa* 3′UTR Deletions to Localize Transcripts to the Germ Plasm in *Xenopus* Oocytes

Species	Localization in *Xenopus* Oocytes
ostariophysan[a]	yes
euteleosts[b]	no
freshwater butterfly fish	yes
SV40 pA	no
Zebrafish *vasa* 3′UTRΔ2	no
Zebrafish *vasa* 3′UTRΔ3	yes
Zebrafish *vasa* 3′UTRΔ4	yes
Xenopus DEADsouth 3′UTR	yes
zebrafish minimal	yes

[a] Species included: zebrafish, Fegrade's danio, and tetra.
[b] Species included: trout, rainbowfish, and medaka.

we generated transgenic zebrafish that express GFP fused to a set of *vasa* 3′UTR deletion constructs (Figure 3A). In order to express these constructs during zebrafish oogenesis, we used the maternally active elongation factor 1α (EF1α) promotor from *Xenopus* (D. Gilmour, personal communication [30]). To analyze the expression pattern of these constructs, we assayed early cleavage stage embryos from transgenic females for localized GFP transcripts. We find that GFP transcripts that are fused to the full-length *vasa* 3′UTR, to the first 334 nucleotides (elements 1 and 2), or to nucleotides 157 to 642 (elements 2 to 4) of *vasa* 3′UTR show a localization pattern that is indistinguishable from the localization of endogenous *vasa* RNA (Figures 3A, 3B, 3E, and 3F, compare to Figure 1Ae). In contrast, GFP transcripts fused to the first 141 nucleotides (element 1) of *vasa* 3′UTR or the SV40 poly A signal do not localize (Figures 3A, 3C, and 3D). Ultrastructural analysis of the subcellular localization of GFP transcripts fused to the *vasa* 3′UTR demonstrates that the reporter transcripts are incorporated into the maternally inherited germ plasm in a similar manner to what we find for injected GFP-*vasa* 3′UTR fusion transcripts in injected *Xenopus* oocytes (compare Figures 3J and 3K). These results show that the 180 nucleotide localization element is also required to localize *vasa* RNA to the germ plasm during zebrafish oogenesis.

To address the question if localized GFP *vasa* 3′UTR fusion transcripts also lead to localized protein expression in the PGCs, we crossed female fish heterozygous for the GFP-*vasa* 3′UTR transgene to wild-type male fish to generate embryos that only carry maternally supplied transcripts from the transgene (Figure 4A). In such embryos, maternally supplied GFP-*vasa* 3′UTR fusion transcripts are detectable within the presumptive PGCs until midsomitogenesis (Figures 3B and 4B). Analysis of GFP translation from these localized transcripts is complicated by maternal GFP protein which is present early on during oogenesis (H.K., unpublished data; Figure 4C). Nevertheless, enrichment of GFP fluorescence in four clusters of two to six cells each is detectable at 50% epiboly. Expression of fluorescent GFP in presumptive PGCs continues to be detectable throughout early development of embryos up to 1.5–2 dpf (see Movie 2 with the Supplementary Material available with this article online). To confirm that cells with enriched GFP fluorescence correspond to presumptive PGCs, embryos were stained for GFP and Vasa protein. These double stainings showed that GFP is specifically enriched in Vasa protein-positive cells (Figure 4D). Furthermore, analysis of transgenic zebrafish that carry truncated *vasa* 3′UTRs lacking the first or last two conserved elements shows that both deletion mutants confer GFP protein expression to the germline (Figures 4F and 4G). These observations demonstrate that the first 334 nucleotides and the last 485 nucleotides of the *vasa* 3′UTR are sufficient to target GFP protein expression to the zebrafish germline, suggesting that the *vasa* 3′UTR can potentially target any protein of interest to the germline of zebrafish. Moreover, the translation of germ plasm targeted GFP-*vasa* 3′UTR fusion transcripts provides a novel in vivo marker for PGCs to study the germ cell migration in zebrafish (Movie 2).

Migratory Behavior of Germ Cells in Zebrafish

The combination of an in vivo marker for the early germline, external development, and transparency of zebrafish embryos allowed us to investigate the behavior of PGCs in a vertebrate during their migration to the future site of the gonadal tissue. We started our time-lapse microscopic analysis at the beginning of gastrulation, because at this stage the PGC fluorescent signal can be clearly distinguished from maternally deposited GFP protein fluorescence. At 50% epiboly, just before gastrulation, PGCs are found in four clusters of about four cells each (Figure 4C). These four clusters are oriented randomly with respect to the dorsal-ventral axis which becomes apparent when the embryonic shield, the zebrafish equivalent of the Spemann organizer, forms at the dorsal side of the embryo. Gastrulation in zebrafish involves the formation of the germ ring and, subsequently, the embryonic shield. This process is caused by complex morphogenetic movements. At the blastoderm margin, cells involute as a rolling cell layer to form the hypoblast or mesendoderm. Cells within this newly formed layer start to stream toward the dorsal side, while cells that have not involuted continue to spread toward the vegetal pole as epiboly continues [31]. During these morphogenetic movements, clusters of PGCs move along with neighboring cells toward the dorsal side of the embryo, aligning at a dorsal-lateral position. From this dorsal-lateral position, the PGC clusters move toward the forming notochord at the level where the first somite will form. This translocation of the four PGC clusters toward the midline involves some active cell movement, since the PGCs orient themselves within the moving stream of cells such that they move along similar routes toward the midline (Figures 5A–5D and Movie 1). As the PGCs reach the notochord, they aggregate into a cluster on each side of the embryo. During somitogenesis, the PGCs are excluded from the forming somitic mesoderm, align more laterally at the level of the second somite (Figures 5E–5H and Movie 2), and partly cease to extend filipodia and assume a round cell shape (Figures 5I, 5J, and 6A and Movies 2, 5, and 6). At the eighth somite stage, the PGCs resume their migratory behavior and leave their position lateral to the second somite and

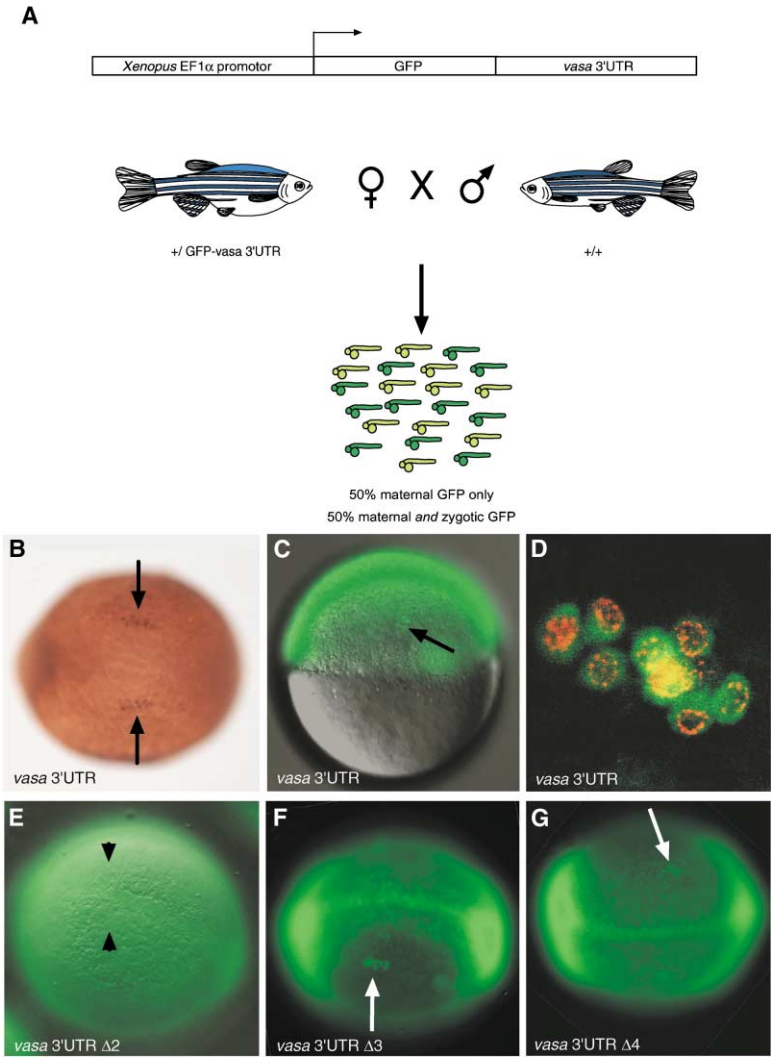

Figure 4. GFP RNA Fused to Zebrafish *vasa* 3′UTR Directs GFP Protein Expression to the Zebrafish Germline

(A) Female zebrafish that are heterozygous for a transgene that encompasses the GFP-*vasa* 3′UTR fusion construct under the *Xenopus* EF1α promoter give rise to two classes of embryos when crossed to wild-type males. Half of the offsprings only inherit maternally supplied GFP-*vasa* 3′UTR transcripts, while the other half inherit both the maternally supplied GFP-*vasa* 3′UTR transcripts and zygotically derived GFP-*vasa* 3′UTR transcripts from the inherited transgene.

(B–G) Embryos that only carry the maternal contribution of GFP-*vasa* 3′UTR RNA distribute these transcripts to the PGCs where it is detectable until midsomitogenesis ([B], arrows indicate GFP RNA positive PGCs; anterior is to the left). Translation of maternally supplied GFP-*vasa* 3′UTR RNA is seen shortly before gastrulation at 50% epiboly ([C], arrow indicates cluster of four PGCs). Cells that translate GFP-*vasa* 3′UTR transcripts correspond to PGCs as is seen in double antibody stainings for GFP (green) and *vasa* protein (red) in a 6 somite embryo (D). Maternally contributed transcripts of GFP-*vasa* 3′UTR deletions 3 and 4 are translated in PGCs ([F], 4 somite stage, and [G], late tailbud stage; arrows indicate GFP protein positive PGC clusters; anterior is to the left), while maternally supplied GFP-*vasa* 3′UTR deletion 1 (data not shown) and 2 ([E], 2 somite stage, arrowheads indicate the position at the notochord where the PGCs reside).

migrate through the lateral plate mesoderm to the eighth somite (Figures 5K, 5L, and 5M–5P and Movies 2 and 3) where they remain until at least 36 hpf when the GFP fluorscence becomes undetectable (Movie 4). During migration to the posterior, PGCs clearly avoid contact with the medially located anlage of the pronephros, while there seems to be no definite lateral limiting tissue (Figures 6C to 6F).

Trailing PGCs are frequently detectable. They either reassociate with the PGC cluster or remain separate within the time period of observation. Such separate PGCs protrude filipodia in all directions and move more randomly and rapidly than their cluster-associated counterparts (5 mm/min compared to 1 mm/min). PGCs become separated from the PGC clusters because they either fall behind or they actively leave the PGC cluster. In the latter case, PGCs frequently circle and return to their initial position within the cluster (Figure 6B). PGCs that are within a cluster appear to explore their surroundings with cell protrusions, move around one another, and appear to touch each other transiently by filipodia (Figure 6A and Movie 6). In summary, PGCs appear to use general morphogenetic cell movements to reach the midline at the level of the second somite, although they actively orient and align themselves within these cell streams. Subsequently, the PGCs actively translocate themselves through the lateral plate mesoderm to the level of the eighth somite.

Discussion

Implications for a Conserved RNA Localization Machinery

In this study, we demonstrate that the zebrafish *vasa* 3′UTR contains a *cis*-acting signal that is sufficient to localize transcripts to the germ plasm in both zebrafish and *Xenopus*. Sequence comparison between different teleosts shows that the *vasa* 3′UTR contains four conserved elements, and, using transgenic zebrafish and the *Xenopus* oocyte injection assay, we show that one of these conserved elements is sufficient for RNA localization to the germ plasm. To understand the mechanism by which this conserved element in the zebrafish *vasa* RNA is localized to the germ plasm in *Xenopus*, we compared the germ plasm localization signals of these two species. In *Xenopus*, the RNAs of *Xcat-2*, a *nanos*

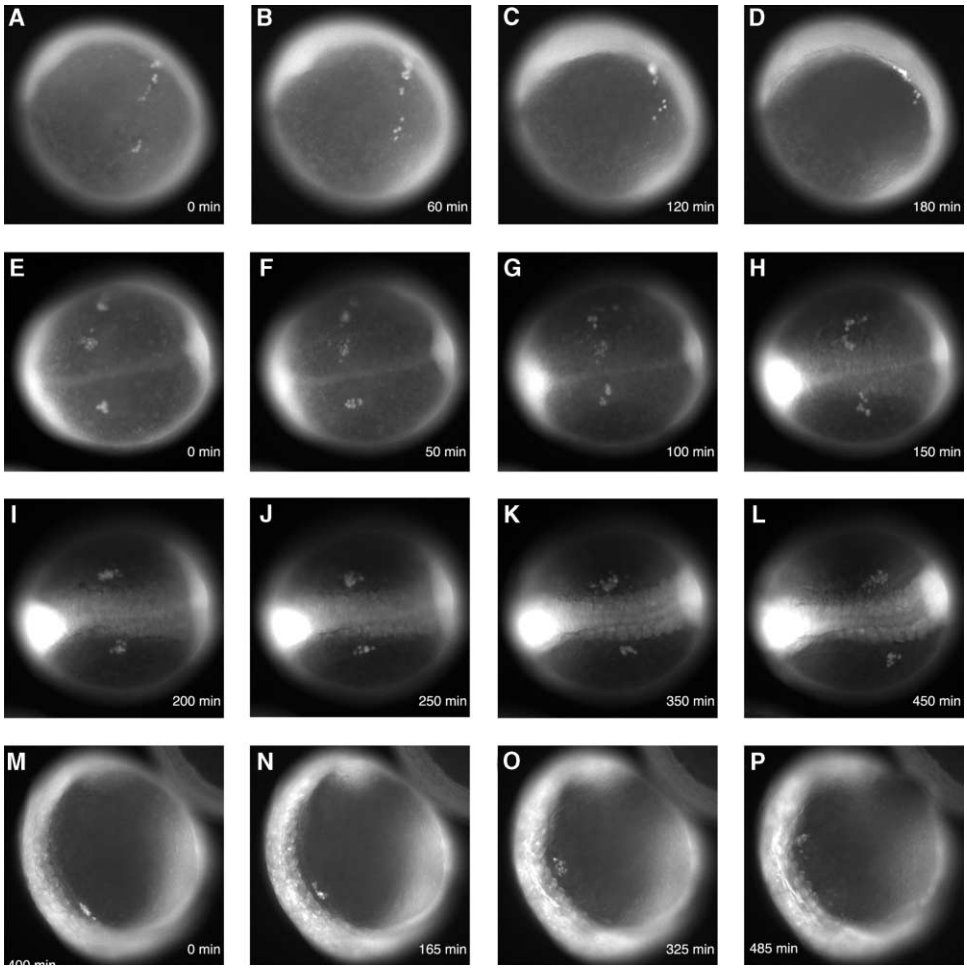

Figure 5. Time-Lapse Microscopy of Migrating PGCs in Zebrafish Embryos

During late epiboly and early tail bud stages, PGCs migrate toward the midline where they form to clusters lateral to the notochord and the forming somites ([A–D], start of time-lapse recording was at the 80% epiboly stage, Movie 1). After clustering and aligning next to the somites, the PGCs migrate posteriorly to the level of the eighth somite ([E–L], start of time-lapse recording was at the early tail bud stage, Movie 2; [M–P], start of time-lapse recording was at the 10 somite stage, Movie 3). The time point when the picture frame was taken is indicated in minutes. In Movies 1–4, frames were recorded every 5 min.

homolog, *Xpat*, a novel protein, *Xdazl*, a homolog of *Drosophila boule*, and the *vasa*-like gene *DEADsouth* are localized to the germ plasm [14, 32–34]. The localization element of *Xcat-2* is composed of two 150 nucleotide elements, and the localization element of *Xpat* maps to its 3′UTR [32, 33, 35]. The localization elements of *Xdazl* and *DEADsouth* have not been reported but are likely to reside within the 3′UTR. Comparing these localization signals to the zebrafish *vasa* localization element, we cannot detect definite similarities in primary or secondary structure. However, we find weak homologies to the zebrafish localization element scattered over 450 nucleotides in the 3′UTR of *DEADsouth*. Using the *Xenopus* oocytes injection assay, we find that this 450 nucleotide region is sufficient for vegetal localization, demonstrating that this region contains a functional localization element. Although the sequence homologies are weak within this region, it is nonetheless likely that the zebrafish localization element is recognized by the same machinery responsible for localization of the endogenous *DEADsouth* RNA. Similarly, we neither can detect definite sequence similarities between the *Ciona intestinalis Ci-DEAD1* 3′UTR and the *Xenopus DEADsouth* 3′UTR nor the ostariophysan germ plasm localization signal, although the *Xenopus* RNA recruiting machinery recognizes all these 3′UTRs as substrates. Since it is unlikely that each of these 3′UTRs is recognized by different *trans*-acting factors, we believe that the competence of the *Xenopus* RNA localization machinery to recruit *vasa*-like transcripts from distant organisms reflects a general conservation of this machinery in lower vertebrates.

The observation that the *vasa* 3′UTR contains three additional conserved sequence elements besides the 180 nucleotide localization element raises the question if they are also important for RNA localization. Although the zebrafish *vasa* RNA localization element is sufficient for localization in *Xenopus* oocytes, we find that localization is more efficient if additional conserved elements are present (compare Figures 3I and 3Q). However, neither the first element nor the last two conserved domains

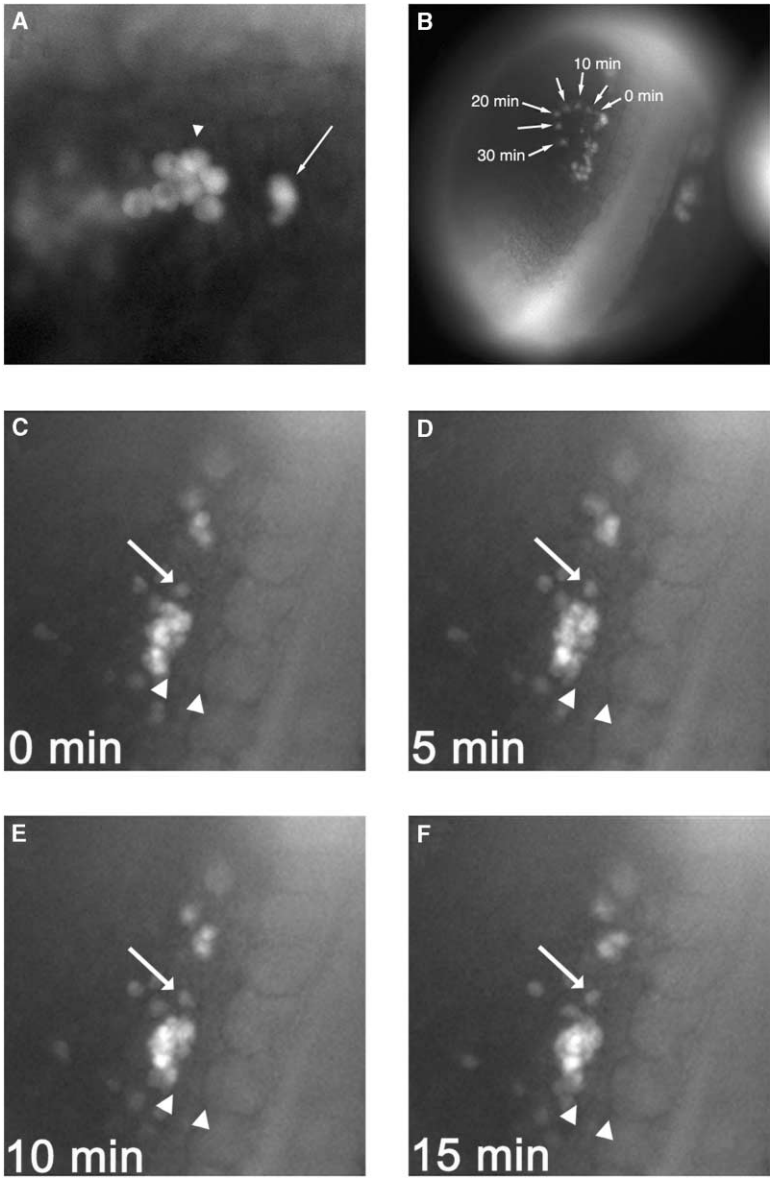

Figure 6. Behavior and Movements of Individual PGCs

(A) See Movies 5 and 6 (one frame every minute). PGCs after aggregation in clusters in a 4 somite embryo. Some PGCs within such a cluster cease moving and assume a round cell shape (arrowhead) in contrast to neighboring PGCs that continue to extend filipodia and move (arrow).

(B) A superposition of the movements of one PGC during the time course of 30 min in a 5 somite embryo. In contrast to PGCs that remain within a cluster, this cell actively leaves the cluster, circles, and returns to the cluster.

(C–F) A 15 min time course of a cluster of PGCs as they migrate posteriorly in a 10 somite embryo, avoiding to enter the pronephros anlage (arrowheads). The arrow points at a cell that moves toward the pronephros (C and D), extends a filipodium (E), and retracts it (F), changing its orientation.

are sufficient for localization in the absence of the second localization element. This suggests that these sequences bear accessory functions, such as RNA anchoring or translational control. We find that the first two elements (nucleotides 1 to 334) and the last three conserved elements (nucleotides 157 to 642) in the zebrafish *vasa* 3′UTR are sufficient to localize and initiate translation in transgenic zebrafish indistinguishable from endogenous *vasa* transcripts, while the most 5′ conserved region alone does not suffice. This suggests that the second element which contains the localization signal also has a function in translational control, although we cannot exclude the possibility of redundant translational control elements.

Evolution of *vasa* RNA Localization in Teleosts

Our comparative approach to identify putative *vasa* RNA localization elements in the *vasa* 3′UTR led to the unexpected observation that *vasa* RNA is not localized in embryos of all teleost species. We find that euteleosts do not localize *vasa* RNA during oogenesis and blastula stage embryogenesis even though they express *vasa* specifically in PGCs during later stages of development. Since we find that maternal *vasa* RNA is localized in oocytes of a basal species, we conclude that the loss of *vasa* RNA localization in euteleosts occurred after the euteleosts and ostariophysan clades separated. This conclusion is supported by our finding that euteleosts lack both a functional localization element and the conserved 180 nucleotide zebrafish localization signal in their *vasa* 3′UTRs, suggesting that the absence of such a localization element is the reason for the loss of maternal *vasa* RNA localization in euteleosts. However, another possibility is that the RNA localization machinery changed during the separation of euteleosts and ostariophysans such that the *vasa* RNA localization element is no longer recognized. One way to distinguish between these hypoth-

eses is to test whether medaka embryos are still able to recognize and recruit transcripts that contain the zebrafish *vasa* RNA localization element.

Moreover, the observation that euteleost fish do not need to localize maternal *vasa* RNA to the germ plasm to specify their germline raises the question if targeted *vasa* gene expression to the germline is essential for germline specification in ostariophysans. Since *vasa* homologs are required for germ cell formation in *Caenorhabditis* and *Drosophila* and for male germ cell proliferation in mice [1–3, 7, 8, 36, 37], it is likely that Vasa protein expression in the germline of teleosts is also essential for germ cell development. Therefore, it is likely that targeting Vasa protein expression to the germline is important, while the mechanism of how to target expression may differ.

There are several possibilities how euteleosts may target Vasa protein expression to the germline. Vasa protein expression may be induced by external signals. Such a mechanism is found in mouse where germ cells are induced by BMP signaling [38, 39]. Alternatively, as *vasa* RNA is present ubiquitously in euteleosts, Vasa protein expression may be induced by selectively protecting *vasa* RNA from degradation in PGCs. Although we cannot exclude the first model, we favor the second for several reasons. First, medaka oocytes and PGCs do indeed contain germ plasm, and this structure may protect *vasa* RNA from degradation [40, 41]. Second, *vasa* RNA distribution in early euteleost embryos shows ubiquitous expression in all blastomeres and successively fades in all cells but the presumptive PGCs (our unpublished data [26]). Third, we find that zebrafish *vasa* RNA which has not aggregated into one of the four main aggregates during blastula stages is lost, presumably due to degradation (data not shown), suggesting a second, independent mechanism for RNA localization in zebrafish. This provides a possible explanation how euteleosts may have lost the ability to localize maternal *vasa* RNA but retained RNA enrichment in PGCs. Mutation of the localization element may have been compensated by the presence of a second, independent localization mechanism. Based on these observations, we believe that in euteleosts Vasa protein expression is targeted to PGCs by selective protection of maternal *vasa* RNA from degradation in presumptive PGCs.

Germ Cell Migration and Behavior in Zebrafish

The specification of PGCs by either intrinsic or extrinsic factors is the first step in establishing the germline in many animals. Once PGCs are set aside, they need to migrate from the place they are born to the future site of the gonads. Although live markers for medaka and mouse PGCs have recently been reported [42, 43], the movement and behavior of PGCs has not been studied in detail in live embryos. Our observation that the zebrafish *vasa* 3′UTR is sufficient to target GFP expression to the germline in transgenic zebrafish provides a novel marker which enabled us to study PGC migration and behavior in detail. The migration in zebrafish can be summarized into two steps. First, PGCs use general gastrulation movements to translocate toward the midline at the level where the first two somites will form. Second, PGCs migrate from the level of the second somite to the level of the eighth somite [15]. The observation of migrating PGCs in live embryos indicates that there exist several guidance cues that help PGCs find their way to the future site of the gonads. Clearly, the region where the first two somites will form provides an attracting molecule as PGCs actively move to this region of the embryo [15]. This is supported by the observation that PGCs which become separated from the PGC cluster frequently return to this intermediate target. Moreover, PGCs which reach this region frequently cease to display migratory behavior and assume a round cell shape, while ectopic germ cells continue to move. Once the eighth somite has formed, the PGCs resume their migration and move posteriorly. Again, the exact timing of this process suggests that PGCs sense a signal that induces this movement. Although we cannot exclude the possibility that the beginning of posterior migration is due to an intrinsic timing mechanism in PGCs themselves, we consider this to be unlikely, since ectopically located germ cells do not show a change in migratory behavior at this developmental time point. Besides attractive signals that appear to direct PGC migration, there are also repulsive signals from the forming pronephros, since PGCs frequently extend filipodia toward this tissue and immediately retract them. This repulsive interaction of PGCs with the pronephros is similar to the guidance of PGCs through the gut to the mesoderm by the repulsive action of the two wunen gene products in *Drosophila* [44, 45]. In summary, zebrafish PGCs undergo at least two phases of migration through the embryo, utilizing both attractive and repulsive guidance cues.

Experimental Procedures

Isolation of *vasa* Orthologs from Different Teleosts

poly(A)$^+$ RNA was enriched from tetra (*Hyphessobryon ecuadoriensis*), trout (*Oncorhynchus mykiss*), medaka (*Oryzias latipes*), rainbow fish (*Melanotaenia fluviatilis*), freshwater butterfly fish (*Pantodon buchholzi*), and *Xenopus* blastula stage embryos or ovaries using TriStar Reagent (Angewandte Gentechnologie Systeme) and oligotex columns (Qiagen) according to the manufacturer's instructions. First-strand cDNA synthesis was performed using Superscript II (Gibco-BRL Life Sciences) with the primer 5′-CCAGTGAGCAGAG TGACGAGGACTCGAGCTCAAGCTTTTTTTTTTTTTTTBN-3′. The DEAD box of the *vasa* orthologs was amplified using the primer pair 5′-ATGGCNTGYGCNCARAC-3′ and 5′-RAANCCCATRTCNARCAT-3′. The 3′ untranslated region was amplified by 3′RACE using taq polymerase (Amersham-Pharmacia) (94°C for 1 min, 58°C for 1 min, 72°C for 3 min, and 30 amplification cycles) and two nested primer pairs. We used the sense primers 5′-TCGGCAGAGGAAAGGTGG-3′ and 5′-AAAGTTCGCCACCTGGTCC-3′ for tetra and medaka, 5′-GCTCA TGGCACCACAGGG-3′ and 5′-CTCTCTTCAGAGAGATGGG-3′ for trout, 5′-TTGGAAGAGGAAAGATCGGC-3′ and 5′-AACTGCGATACC TGGTACTGG-3′ for rainbow fish, and 5′-TTGGAAGAGGAAAGGTT GGC-3′ and 5′-AAGCTTCGCTACCTTGTACTGG-3′ for freshwater butterfly fish. As antisense primers, we used 5′-CCAGTGAGCAGAG TGACG-3′ and 5′-GAGGACTCGAGCTCAAGC-3′. The *vasa* ortholog from carp (*Cyprinus carpio*) was isolated screening a phage library [18] with a zebrafish *vasa* 384 nucleotide fragment that encodes the DEAD box domain (nucleotides 952 to 1336). The *Xenopus DEADsouth* 3′UTR fragment (corresponding to nucleotides 1564 to 2078) was amplified using the primers 5′-GGCCCTCGAGCAAATGAACTT TTGTTAAGGG-3′ and 5′-GGCCTCTAGACAAGTGCTTCAGTCA GCC-3′. The *Ciona intestinalis* Ci-DEAD1 3′UTR was amplified using the primers 5′-CTCTTATTGGAATTGAAAAG-3′ and 5′-AATAACGAA GTGTTGTATTT-3′. Sequence alignment was performed using Megalign software (Clustal Method) (DNAStar Inc). Evolutionary dis-

tances among the *vasa* orthologs were calculated using PAUP software (Sinauer Association, David L. Swofford). These calculations were based on changes in the C-terminal coding region (corresponding to amino acids 317 to 688 of the zebrafish Vasa protein). The accession numbers for the *vasa* sequences of tetra, Fegrade's danio, zebrafish, carp, trout, rainbow fish, madaka, and freshwater butterfly fish are AF479821, AF251800, AB005147, AF479820, AF479825, AF479824, AF479822, and AF479823, respectively.

Secondary structure predictions of teleost *vasa* 3′UTRs were performed using the MFOLD program [19]. *vasa* 3′UTR regions that fold into similar structures over a range of the six to ten lowest energy predictions were defined as stable secondary structures. Nucleotide regions of stable secondary structures were noted for the zebrafish *vasa* 3′UTR and compared to teleost *vasa* 3′UTR regions that also form stable secondary structures. Such a comparison identified four regions of conserved secondary structure elements in the ostariophysan *vasa* 3′UTRs, while no conserved secondary structure elements were discernible between zebrafish and euteleost or butterfly fish *vasa* 3′UTR.

In Situ Hybridization, Antibody Stainings, and Electron Microscopy

For analyzing *vasa* RNA distribution in teleosts and GFP RNA in transgenic zebrafish, we performed in situ hybridization as described in Ober and Schulte-Merker [20]. For colocalization of Vasa protein and GFP protein, embryos were stained as described previously [13]. Anti-Vasa serum (K12-3, [13]) was used at a dilution 1:5000 and anti-GFP serum (DPC Biermann) at a dilution of 1:500 and detected using donkey anti-rabbit-Cy3 (Dianova) and donkey anti-goat Alexa 488 (Molecular Probes). Sense and antisense *vasa* RNA probes were synthesized from the 3′UTR of the different telosts (corresponding to nucleotides 2222–2865 of *vasa* cDNA from zebrafish, nucleotides 1153–1779 of *vasa* from Fegrade's danio, nucleotides 1195–1841 of *vasa* from carp, nucleotides 1192–1731 of *vasa* from tetra, nucleotides 1189–1450 of *vasa* from medaka, nucleotides 1201–1507 of *vasa* from rainbow fish, nucleotides 1189–1805 of *vasa* from trout, and nucleotides 1183–1513 of *vasa* from fresh water butterfly fish).

For GFP RNA detection on electron microscopy sections, embryos were stained as described above. The signal was detected using a solution of 0.2 mg/ml DAB (Boehringer Mannheim), 1% $(NH_4)_2Ni_2(I,II)(SO_4)_2$ (Sigma), and 1 mM Imidazol (Sigma) in PBST. All sections were contrasted using uranyl acetate and osmium tetroxide and inspected using a Philips TEM 10 electron microscope.

Generation of Transgenic Animals

Part of the *Xenopus* EF1α promotor (0.5 kb) [21] was cloned as an SalI/HindIII fragment upstream of GFP, followed by the SV40 terminator (C.-B. Chien and D.T. Gilmour, personal communication). Different parts of zebrafish *vasa* 3′UTR were amplified by PCR (Figure 5A) and inserted in this vector downstream of GFP and upstream of the SV40 terminator. This plasmid was used to transform one-cell eggs as described [22]. For the generation of transgenic flies, we used the p(CasPer) vector expressing the transgenic RNA and protein under the control of the maternal tubulin gene promotor.

RNA Localization Assay in *Xenopus* Oocytes

GFP fused to the different parts of the zebrafish *vasa* 3′UTR (Figure 5A), to the *vasa* 3′UTRs from the seven teleost species, and to a *Xenopus DEADsouth* 3′UTR fragment (nucleotides 1564 to 2069, accession number AF190623) was cloned as a BamHI/XbaI fragment into pCS2+ [23, 24] and in vitro transcribed using the messenger machine kit (Ambion). Quality and quantity of RNA was controlled by RNA gel analysis. For injections, 5 nl of a 200 ng/μl RNA solution was used. Unpigmented stage II to III oocytes were isolated, collagenase treated, injected on agar plates, and cultured in modified Barth solution (88 mM NaCl, 1 mM KCl, 2.4 mM $NaHCO_3$, 0.82 mM $MgSO_4$, 0.41 mM $CaCl_2$, 0.33 mM $Ca(NO_3)_2$, 10 mM HEPES, 10 mg/l benzylpenicillin, 10 mg/l streptomycinsulfate [pH 7.5]) for 1 day at 16°C and fixed in MEMFA (0.1 M MOPS, 2 mM EGTA, 3.7% formaldehyde, 1 mM $MgSO_4$ [pH 7.4]). Since we find that older pigmented oocytes (stage IV to VI) are not competent to localize injected transcripts to the germ plasm, pigmentation cannot be used as a marker for the animal pole (data not shown). To mark the animal-vegetal axis in unpigmented oocytes, we performed a double in situ hybridization against the endogenous germ plasm component *DEADsouth* and the injected GFP fusion transcripts. Alternatively, we used a mitochonrial dye (MitoTracker, Molecular Probes) to stain the vegetally localized mitochondrial cloud before in situ hybridization against the injected GFP fusion transcripts. Since the mitochondrial dye and the in situ hybridization dye BCIP/INT (sigma) are unstable in plastic embeddings, we physically marked the vegetal pole by inserting a little glass needle next to it before embedding in epon (Roth). Whole-mount in situ hybridized oocytes and 10 μm sections thereof were assayed for vegetal RNA localization. Vegetal pole identification also was done by inspecting electron microscopic sections to confirm colocalization of the in situ hybridization signal and the mitochondrial cloud.

Time-Lapse Recordings

For time-lapse analysis, embryos were dechorionated and mounted in 0.8% agarose and sealed with wax. Migration of PGCs was followed using a Zeiss Axioplan 2 setup connected to a Hamamatsu digital camera. Image sequences were processed using MetaMorph software (universal imaging corporation provided by Visitron System GmbH). If not stated otherwise, frames were recorded in four different focal planes every 5 min.

Supplementary Material

Supplementary Material including movies showing the migration of PGCs can be found online at http://images.cellpress.com/supmat/supmatin.htm.

Acknowledgments

We are grateful for the excellent technical assistance of Christian Werz, Brigitte Sailer, and Birgitta Latemann. We would like thank Kai-Erik Witte for advice on teleost phylogeny and Darren Gilmour for pointing out the maternal contribution of the EF1α promotor and the gift of plasmids and transgenic fish. We thank David Keys and Michael Levine for the *Ciona intestinalis* phage library. Special thanks to Frank Schnorrer and Kerstin Bohmann for suggestions and discussions. We thank Henri Strohband, Heinrich Gewinner, Ralf Britz, Roland Lusmöller, and Jochen Wittbrodt for fish material. Additionally, we are grateful to Henry Roehl, Frank Schnorrer, Elke Ober, Florian Maderspacher, Jürg Müller, Darren Gilmour, and Jörg Grosshans for critical comments on the manuscript. H.K. thanks Jochen Wittbrodt for hospitality and advice on medaka. This work was supported by the Max-Planck Society. H.K. was supported by a Boehringer-Ingelheim predoctoral fellowship.

Received: October 12, 2001
Revised: January 2, 2002
Accepted: January 18, 2002
Published: March 19, 2002

References

1. Schüpbach, T., and Wieschaus, E. (1986). Maternal-effect mutations altering the anterior-posterior pattern of the Drosophila embryo. Roux's Arch. Dev. Biol. *195*, 302–317.
2. Hay, B., Jan, L.Y., and Jan, Y.N. (1988). A protein component of *Drosophila* polar granules is encoded by vasa and has extensive sequence similarity to ATP-dependent helicases. Cell *55*, 577–587.
3. Lasko, P.F., and Ashburner, M. (1988). The product of the Drosophila gene vasa is very similar to eukaryotic initiation factor-4A. Nature *335*, 611–617.
4. Raz, E. (2000). The function and regulation of vasa-like genes in germ-cell development. Genome Biol. *1*, reviews1017.
5. Wylie, C. (2000). Germ cells. Curr. Opin. Genet. Dev. *10*, 410–413.
6. Hay, B., Ackerman, L., Barbel, S., Jan, L.Y., and Jan, Y.N. (1988). Identification of a component of Drosophila polar granules. Development *103*, 625–640.
7. Gruidl, M.E., Smith, P.A., Kuznicki, K.A., McCrone, J.S., Kirchner, J., Roussell, D.L., Strome, S., and Bennett, K.L. (1996).

Multiple potential germ-line helicases are components of the germ-line- specific P granules of Caenorhabditis elegans. Proc. Natl. Acad. Sci. USA *93*, 13837–13842.

8. Kuznicki, K.A., Smith, P.A., Leung-Chiu, W.M., Estevez, A.O., Scott, H.C., and Bennett, K.L. (2000). Combinatorial RNA interference indicates GLH-4 can compensate for GLH-1; these two P granule components are critical for fertility in C. elegans. Development *127*, 2907–2916.
9. Strome, S., and Wood, W.B. (1982). Immunofluorescence visualization of germ-line-specific cytoplasmic granules in embryos, larvae, and adults of Caenorhabditis elegans. Proc. Natl. Acad. Sci. USA *79*, 1558–1562.
10. Roussell, D.L., and Bennett, K.L. (1993). glh-1, a germ-line putative RNA helicase from Caenorhabditis, has four zinc fingers. Proc. Natl. Acad. Sci. USA *90*, 9300–9304.
11. Yoon, C., Kawakami, K., and Hopkins, N. (1997). Zebrafish vasa homologue RNA is localized to the cleavage planes of 2- and 4-cell-stage embryos and is expressed in the primordial germ cells. Development *124*, 3157–3165.
12. Olsen, L.C., Aasland, R., and Fjose, A. (1997). A vasa-like gene in zebrafish identifies putative primordial germ cells. Mech. Dev. *66*, 95–105.
13. Knaut, H., Pelegri, F., Bohmann, K., Schwarz, H., and Nusslein-Volhard, C. (2000). Zebrafish vasa RNA but not its protein is a component of the germ plasm and segregates asymmetrically before germline specification. J. Cell Biol. *149*, 875–888.
14. MacArthur, H., Houston, D.W., Bubunenko, M., Mosquera, L., and King, M.L. (2000). DEADSouth is a germ plasm specific DEAD-box RNA helicase in xenopus related to eIF4A. Mech. Dev. *95*, 291–295.
15. Weidinger, G., Wolke, U., Koprunner, M., Klinger, M., and Raz, E. (1999). Identification of tissues and patterning events required for distinct steps in early migration of zebrafish primordial germ cells. Development *126*, 5295–5307.
16. Whitington, P.M., and Dixon, K.E. (1975). Quantitative studies of germ plasm and germ cells during early embryogenesis of Xenopus laevis. J. Embryol. Exp. Morphol. *33*, 57–74.
17. Braat, A.K., Zandbergen, T., Van de Water, S., Goos, H.J.T., and Zivkovic, D. (1999). Characterization of zebrafish primordial germ cells: morphology and early distribution of vasa RNA. Dev. Dyn. *216*, 153–167.
18. Stevens, C.J.M., Kronnie, G., Samallo, J., Schipper, H., and Stroband, H.W.J. (1996). Isolation of carp cDNA clones, representing developmentally-regulated genes, using a subtractive-hybridization strategy. Roux's Arch. Dev. Biol. *205*, 460–467.
19. Zuker, M. (1989). On finding all suboptimal foldings of an RNA molecule. Science *244*, 48–52.
20. Ober, E.A., and Schulte-Merker, S. (1999). Signals from the yolk cell induce mesoderm, neuroectoderm, the trunk organizer, and the notochord in zebrafish. Dev. Biol. *215*, 167–181.
21. Johnson, A.D., and Krieg, P.A. (1995). A Xenopus laevis gene encoding EF-1 alpha S, the somatic form of elongation factor 1 alpha: sequence, structure, and identification of regulatory elements required for embryonic transcription. Dev. Genet. *17*, 280–290.
22. Gilmour, D.T., Jessen, J.R., and Lin, S. (2001). Manipulating Gene Expression in the Zebrafish. In Zebrafish: A Practical Approach, C. Nüsslein-Volhard and R. Dahm, eds. (Oxford: Oxford University Press), in press.
23. Turner, D.L., and Weintraub, H. (1994). Expression of achaete-scute homolog 3 in Xenopus embryos converts ectodermal cells to a neural fate. Genes Dev. *8*, 1434–1447.
24. Rupp, R.A., Snider, L., and Weintraub, H. (1994). Xenopus embryos regulate the nuclear localization of XMyoD. Genes Dev. *8*, 1311–1323.
25. Pelegri, F., Knaut, H., Maischein, H.M., Schulte-Merker, S., and Nusslein-Volhard, C. (1999). A mutation in the zebrafish maternal-effect gene nebel affects furrow formation and vasa RNA localization. Curr. Biol. *9*, 1431–1440.
26. Shinomiya, A., Tanaka, M., Kobayashi, T., Nagahama, Y., and Hamaguchi, S. (2000). The vasa-like gene, olvas, identifies the migration path of primordial germ cells during embryonic body formation stage in the medaka, Oryzias latipes. Dev. Growth Differ. *42*, 317–326.
27. Fink, S.V., and Fink, W.L. (1996). Interrelationship of ostariophysan fishes (Teleostei). In Interrelationships of Fishes, M.L.J. Stiassny, L.R. Parenti, and G.D. Johnson, eds. (San Diego: Academic Press), pp. 209–245.
28. Yoshizaki, G., Sakatani, S., Tominaga, H., and Takeuchi, T. (2000). Cloning and characterization of a vasa-like gene in rainbow trout and its expression in the germ cell lineage. Mol. Reprod. Dev. *55*, 364–371.
29. MacArthur, H., Bubunenko, M., Houston, D.W., and King, M.L. (1999). Xcat2 RNA is a translationally sequestered germ plasm component in Xenopus. Mech. Dev. *84*, 75–88.
30. Linney, E., Hardison, N.L., Lonze, B.E., Lyons, S., and DiNapoli, L. (1999). Transgene expression in zebrafish: A comparison of retroviral-vector and DNA-injection approaches. Dev. Biol. *213*, 207–216.
31. Kimmel, C.B., Ballard, W.W., Kimmel, S.R., Ullmann, B., and Schilling, T.F. (1995). Stages of embryonic development of the zebrafish. Dev. Dyn. *203*, 253–310.
32. Zhou, Y., and King, M.L. (1996). RNA transport to the vegetal cortex of Xenopus oocytes. Dev. Biol. *179*, 173–183.
33. Hudson, C., and Woodland, H.R. (1998). Xpat, a gene expressed specifically in germ plasm and primordial germ cells of Xenopus laevis. Mech. Dev. *73*, 159–168.
34. Houston, D.W., Zhang, J., Maines, J.Z., Wasserman, S.A., and King, M.L. (1998). A Xenopus DAZ-like gene encodes an RNA component of germ plasm and is a functional homologue of Drosophila boule. Development *125*, 171–180.
35. Kloc, M., Bilinski, S., Pui-Yee Chan, A., and Etkin, L.D. (2000). The targeting of Xcat2 mRNA to the germinal granules depends on a cis-acting germinal granule localization element within the 3′UTR. Dev. Biol. *217*, 221–229.
36. Tanaka, S.S., Toyooka, Y., Akasu, R., Katoh-Fukui, Y., Nakahara, Y., Suzuki, R., Yokoyama, M., and Noce, T. (2000). The mouse homolog of Drosophila Vasa is required for the development of male germ cells. Genes Dev. *14*, 841–853.
37. Lehmann, R., and Nusslein-Volhard, C. (1991). The maternal gene nanos has a central role in posterior pattern formation of the Drosophila embryo. Development *112*, 679–691.
38. Lawson, K.A., Dunn, N.R., Roelen, B.A., Zeinstra, L.M., Davis, A.M., Wright, C.V., Korving, J.P., and Hogan, B.L. (1999). Bmp4 is required for the generation of primordial germ cells in the mouse embryo. Genes Dev. *13*, 424–436.
39. Ying, Y., Liu, X.M., Marble, A., Lawson, K.A., and Zhao, G.Q. (2000). Requirement of Bmp8b for the generation of primordial germ cells in the mouse. Mol. Endocrinol. *14*, 1053–1063.
40. Hamaguchi, S. (1985). Changes in the morphology of the germinal dense bodies in primordial germ cells of the teleost, Oryzias latipes. Cell Tissue Res. *240*, 669–673.
41. Satoh, N. (1974). An ultrastructural study of sex differentiation in the teleost Oryzias latipes. J. Embryol. Exp. Morphol. *32*, 195–215.
42. Tanaka, M., Kinoshita, M., Kobayashi, D., and Nagahama, Y. (2001). Establishment of medaka (Oryzias latipes) transgenic lines with the expression of green fluorescent protein fluorescence exclusively in germ cells: A useful model to monitor germ cells in a live vertebrate. Proc. Natl. Acad. Sci. USA *98*, 2544–2549.
43. Anderson, R., Copeland, T.K., Scholer, H., Heasman, J., and Wylie, C. (2000). The onset of germ cell migration in the mouse embryo. Mech. Dev. *91*, 61–68.
44. Zhang, N., Zhang, J., Purcell, K.J., Cheng, Y., and Howard, K. (1997). The Drosophila protein Wunen repels migrating germ cells. Nature *385*, 64–67.
45. Starz-Gaiano, M., Cho, N.K., Forbes, A., and Lehmann, R. (2001). Spatially restricted activity of a Drosophila lipid phosphatase guides migrating germ cells. Development *128*, 983–991.

Accession Numbers

The sequences reported in this study have been submitted to GenBank with the accession numbers AF479820, AF479821, AF479822, AF479823, AF479824, and AF479825.